Rice

RESEARCH Open Access

GWAS and Candidate Gene Prediction of Elemental Accumulation Traits in Rice Using a Multiparental Population

Qian Zhang[1], Tomoyuki Furuta[1], Kazunari Kashihara[1], Daisuke Ogawa[2], Junichi Yonemaru[3], Jian Feng Ma[1] and Toshio Yamamoto[1*]

Abstract

Rice plants accumulate essential elements to sustain physiological processes during growth and development and to ensure the nutritional quality of the grain as a food source. However, the genetic basis of elemental accumulation and the interrelationships among elemental concentrations across different tissues remain poorly understood. To conduct breeding aimed at improving the absorption characteristics of multiple interrelated elements, genetic analysis using experimental populations that retain diversity while sharing the genetic background of cultivated varieties is effective. Here we show genetic variations in the concentrations of 13 elements (P, K, Ca, Mg, As, Cd, Cr, Cu, Fe, Mo, Mn, Ni, and Zn) in rice straw at the flowering stage and grain at the mature stage using a multi-parent advanced generation inter-cross (MAGIC) population that derived from eight cultivars including both Japonica and Indica. Comprehensive evaluation of the correlation coefficients revealed divergences in the association between grain and straw for several combinations of elements. Haplotype-based genome-wide association studies (GWAS) identified 51 and 53 quantitative trait loci (QTLs) in straw and grain, respectively. In total, the 104 QTLs were grouped into 19 clusters and 60 independent QTLs. By leveraging the haplotype information from the MAGIC population, 52 candidate genes associated with the accumulation of Ca, Mg, Cd, Cu, Fe, and Mo were efficiently predicted from these QTLs, including both previously reported and novel genes. Among them, *OsMOT1;1* encoding a molybdenum transporter, was predicted to be within a QTL associated with Mo accumulation in grain on chromosome 8. *OsACA9*, a homolog of autoinhibited Ca^{2+}-ATPases, was predicted within a QTL related to Ca accumulation in straw on chromosome 2. In addition, an unidentified gene, *OsCML6*, which is presumed to be involved in calcium signaling, was predicted to be a candidate for a Ca-accumulation QTL on chromosome 11. These findings offer insights into haplotypes and putative genes associated with element accumulation and trait interrelationships, providing valuable information for optimizing plant growth and enhancing grain nutritional quality in rice breeding programs.

Keywords Rice, *Oryza sativa* L., Multi-parent advanced generation inter-cross population, Element accumulation, GWAS, QTL

*Correspondence:
Toshio Yamamoto
yamamo101040@okayama-u.ac.jp
[1]Institute of Plant Science and Resources, Okayama University, 2-20-1 Chuo, Kurashiki 710-0046, Japan
[2]Institute of Crop Science, National Agriculture and Food Research Organization, 2-1-2 Kannondai, Tsukuba 305-8518, Japan
[3]Research Center for Agricultural Information Technology, National Agriculture and Food Research Organization, 3-1-1 Kannondai, Tsukuba 305-8517, Japan

Background

Rice (*Oryza sativa* L.) is one of the most important and well-established crops, serving as a staple food for nearly half of the world's population (Khush 2005). The success of the "Green Revolution" in the mid-20th century was a landmark event that allowed the world to see the utility of scientific breeding (Evenson and Gollin 2003; Pingali 2012). However, recent climate changes and fluctuations in global agricultural markets have generated numerous new concerns, necessitating the development of rice varieties with diverse and improved traits. One such concern is inefficient elemental uptake and imbalances in soil nutrient utilization associated with soil degradation, which often limit rice productivity (Ye et al. 2024).

Soil contains elements that are essential for plant growth and can be categorized based on plant requirements. Macroelements, which are required in large amounts for plant metabolism and growth, include C, N, P, K, Ca, Mg, and S (Hawkesford 2012). Trace elements, which are required in minimal quantities, account for 5 to 200 ppm, or less than 0.02% dry weight of plants and include Fe, Mn, B, Zn, Cu, Cl, Ni and Mo (Kathpalia 2018). Some of these elements are basic components of the plant protoplasm and components or activators of enzymes, whereas others can regulate protoplasmic membrane permeability, participate in buffer systems, and maintain cell permeability to sustain normal life activities (Taiz 2015). Lack of these elements causes physiological imbalances, affects growth and development, and manifests as specific symptoms of deficiency. In addition, both beneficial and toxic elements are present in soil. Beneficial elements can promote the growth and development of certain plants. For example, Si enhances the growth of melon and vegetables, thereby improving their resistance (Ma and Yamaji 2006). Toxic elements, such as Cd and As, not only impede plant growth but are also harmful to humans (Uchimiya et al. 2020). Beyond their importance for plant physiology, the elemental composition of rice grains directly affects human nutrition and food safety. Extensive datasets linking variations in grain element concentrations with potential dietary relevance are available in food composition databases (USDA FoodData Central, https://fdc.nal.usda.gov/). Food safety standards also specify limits for toxic elements (Codex 2025). Genetic variation in rice elements significantly influences both aspects. Therefore, elucidating the physiological roles of mineral elements and the genetic basis of their uptake and transport in plants can inform optimized nutrient management and breeding strategies to enhance yield and improve crop quality.

There is no doubt that crop genomic information, which is being rapidly revealed, makes an important contribution to breeding. After the rice genome was decoded (IRGSP 2005), the isolation and functional analysis of a large number of genes have advanced notably (Chen et al. 2022). This information has not only contributed to plant sciences but has also set a new trend in rice breeding. In particular, DNA marker-assisted breeding has greatly simplified the process of evaluating traits, which has been a challenge in conventional breeding, by increasing selection efficiency and reducing selection times (Yamamoto et al. 2009). However, the genomic history of rice breeding has revealed a narrow genetic diversity of current rice varieties, which will become a potential genetic resource for future breeding (Yonemaru et al. 2012). To ensure sustainable genetic improvement, new breeding techniques are required to maximize the potential diversity offered by combinations of breeding lines.

To expand genetic diversity by collapsing the genome structure in a crossbreeding population, a multiparent advanced generation inter-cross (MAGIC) population, consisting of multiple crosses derived from three or more founder varieties, has been proposed (Cavanagh et al. 2008; Kover et al. 2009). Since MAGIC populations have the advantage of QTL detection accuracy compared to single-cross populations and can produce gene combinations as diverse as outcrossing populations, they have been developed in many crop species such as tomatoes (Pascual et al. 2015), cowpea (Huynh et al. 2018), maize (Dell'Acqua et al. 2015), cotton (Islam et al. 2016), wheat (Huang et al. 2012; Mackay et al. 2014), barley (Sannemann et al. 2015), eggplant (Mangino et al. 2022), and rice (Bandillo et al. 2013; Meng et al. 2015; Ogawa et al. 2018a). The multifounder design in the MAGIC population ensures that each parent contributes to at least one target trait and that several parents may harbor favorable alleles for the same trait. This strategy greatly increases the diversity and combinations of functional alleles, thereby substantially enriching genetic diversity. Wang P. et al. (2024) demonstrated that the MAGIC population has great potential for exploring novel alleles of days to heading in natural or breeding rice varieties.

Most genetic analyses of elemental accumulation in rice have been conducted using mutants and distantly related varieties exhibiting extreme phenotypes. Extensive genetic and physiological studies comparing the functions of these alleles with those of the currently cultivated varieties have elucidated the molecular mechanisms underlying element uptake and translocation. However, to fully utilize this genetic information in practical breeding, it is necessary to understand the variation in the number and types of genes underlying these genetic mechanisms within the natural variations of rice currently used in crossbreeding programs. In this context, comprehensive genetic analysis using MAGIC, which comprises diverse varieties within a target region, is considered a highly effective approach. The elemental contents of plant tissues are thought to be subject to

Table 1 Summary of significant QTLs (FDR ≤ 0.1) involving elemental concentrations in rice grain and straw using the MAGIC population

Grain Element	QTL name	SNP marker	−log10(p)	FDR	Straw Element	QTL name	SNP marker	−log10(p)	FDR
	q21GCd3-1	Chr3_27703252	2.93	***0.0453***		*q21SCa1-1*	Chr1_30341513	2.62	0.0718
	q21GCd3-2	Chr3_30422353	3.57	***0.0209***		*q21SCa1-2*	Chr1_35886973	2.34	0.0906
	q21GCd4-1	Chr4_1015760	2.42	0.0916		*q21SCa2-1*	Chr2_1003070	4.38	***0.0358***
	q21GCd4-2	Chr4_4598416	2.46	0.0879		*q21SCa2-2*	Chr2_9936760	3.05	***0.0423***
	q21GCd5	Chr5_24799047	2.38	0.0944		*q21SCa2-3*	Chr2_12082859	2.67	0.0718
Cd	*q21GCd6-1*	Chr6_818002	2.93	***0.0453***	Ca	*q21SCa2-4*	Chr2_28817978	2.82	0.0553
	q21GCd6-2	Chr6_1947565	4.58	***0.0191***		*q21SCa6-1*	Chr6_906853	3.44	***0.0358***
	q21GCd6-3	Chr6_26383319	2.46	0.0879		*q21SCa6-2*	Chr6_27609600	3.75	***0.0358***
	q21GCd7-1	Chr7_5852706	4.38	***0.0191***		*q21SCa7*	Chr7_25637166	2.77	0.0618
	q21GCd7-2	Chr7_21290846	2.37	0.0944		*q21SCa10*	Chr10_772038	2.31	0.0942
	q21GCd9	Chr9_13860903	2.64	0.0700		*q21SCa11*	Chr11_20019091	3.97	***0.0358***
	q21GCd11-1	Chr11_7024776	3.23	***0.0263***		*q21SMg1*	Chr1_38968519	2.90	0.0646
	q21GCd11-2	Chr11_21722693	2.41	0.0916		*q21SMg2*	Chr2_27493441	2.07	0.0924
	q21GCd11-3	Chr11_24809829	2.52	0.0791		*q21SMg3-1*	Chr3_8182099	2.02	0.0968
	q21GCd12	Chr12_3481562	2.38	0.0944		*q21SMg3-2*	Chr3_30422353	2.34	0.0769
Cu	*q21GCu1-1*	Chr1_3465892	2.81	0.0682		*q21SMg3-3*	Chr3_33913703	3.61	0.0646
	q21GCu1-2	Chr1_30397482	3.39	0.0610		*q21SMg4*	Chr4_23235680	2.75	0.0646
	q21GCu2	Chr2_23652007	3.01	0.0610	Mg	*q21SMg5-1*	Chr5_903828	2.94	0.0646
	q21GCu4-1	Chr4_5005293	2.92	0.0649		*q21SMg5-2*	Chr5_20100264	2.21	0.0824
	q21GCu4-2	Chr4_32654876	2.43	0.0917		*q21SMg6-1*	Chr6_2898917	2.03	0.0965
	q21GCu6-1	Chr6_272094	2.80	0.0682		*q21SMg6-2*	Chr6_25127567	2.87	0.0646
	q21GCu6-2	Chr6_23133577	2.56	0.0805		*q21SMg7-1*	Chr7_4139442	3.33	0.0646
	q21GCu7	Chr7_5775203	3.58	0.0610		*q21SMg7-2*	Chr7_23879876	2.68	0.0664
	q21GCu11	Chr11_19450668	3.04	0.0610		*q21SMg8-1*	Chr8_1152627	2.44	0.0762
	q21GFe1	Chr1_1928663	2.17	0.0983		*q21SMg8-2*	Chr8_27896450	2.29	0.0786
	q21GFe2	Chr2_22089977	2.17	0.0983		*q21SMg9-1*	Chr9_16610541	2.05	0.0942
	q21GFe3	Chr3_211120	2.50	0.0807		*q21SMg9-2*	Chr9_21306262	2.94	0.0646
	q21GFe4-1	Chr4_11760	4.09	0.0634		*q21SMg10-1*	Chr10_87974	2.32	0.0776
	q21GFe4-2	Chr4_7380693	2.24	0.0974		*q21SMg10-2*	Chr10_19811172	2.37	0.0762
	q21GFe4-3	Chr4_8125665	2.86	0.0634		*q21SMg11-1*	Chr11_1293419	3.51	0.0646
	q21GFe4-4	Chr4_16598461	3.37	0.0634		*q21SMg11-2*	Chr11_7666770	2.07	0.0931
Fe	*q21GFe6-1*	Chr6_2898917	2.16	0.0983		*q21SMn1*	Chr1_22617559	2.77	0.0973
	q21GFe6-2	Chr6_11885263	2.93	0.0634		*q21SMn2-1*	Chr2_9619	2.99	0.0973
	q21GFe6-3	Chr6_16804756	2.17	0.0983		*q21SMn2-2*	Chr2_3370339	3.72	0.0768
	q21GFe6-4	Chr6_18841514	2.37	0.0891		*q21SMn4*	Chr4_19629130	3.51	0.0973
	q21GFe6-5	Chr6_26742584	2.26	0.0974	Mn	*q21SMn5*	Chr5_27586439	4.52	***0.0444***
	q21GFe7-1	Chr7_3468635	2.60	0.0737		*q21SMn6-1*	Chr6_3322080	2.64	0.0995
	q21GFe7-2	Chr7_5208158	3.18	0.0634		*q21SMn6-2*	Chr6_27061467	2.88	0.0973
	q21GFe7-3	Chr7_14863454	2.25	0.0974		*q21SMn11-1*	Chr11_3788078	2.95	0.0973

Table 1 (continued)

Grain Element	QTL name	SNP marker	−log10(p)	FDR	Straw Element	QTL name	SNP marker	−log10(p)	FDR
	q21GFe7-4	Chr7_27803788	2.31	0.0919		*q21SMn11-2*	Chr11_19284207	3.03	0.0973
	q21GFe8	Chr8_3960499	2.12	0.0995		*q21SMo1*	Chr1_28965344	6.39	***0.0005***
	q21GFe12-1	Chr12_4687453	3.48	0.0634		*q21SMo2-1*	Chr2_3964230	2.40	0.0827
	q21GFe12-2	Chr12_10465894	3.09	0.0634		*q21SMo2-2*	Chr2_16095083	2.30	0.0966
Mn	*q21GMn5*	Chr5_25805065	3.82	0.0670		*q21SMo2-3*	Chr2_22180762	2.39	0.0838
	q21GMo1	Chr1_26290272	2.74	0.0530		*q21SMo3*	Chr3_211120	2.29	0.0974
	q21GMo2	Chr2_35261376	2.43	0.0936	Mo	*q21SMo4*	Chr4_7150241	2.31	0.0959
	q21GMo3	Chr3_23153229	2.40	0.0969		*q21SMo6-1*	Chr6_139521	3.33	***0.0207***
	q21GMo6	Chr6_26742584	2.54	0.0785		*q21SMo6-2*	Chr6_3541729	2.35	0.0912
Mo	*q21GMo7-1*	Chr7_4926246	5.36	***0.0050***		*q21SMo9*	Chr9_22419659	2.28	0.0986
	q21GMo7-2	Chr7_19693968	3.12	***0.0266***		*q21SMo10*	Chr10_18064070	3.57	***0.0164***
	q21GMo8	Chr8_72552	3.60	***0.0132***		*q21SMo11*	Chr11_23755723	3.60	***0.0164***
	q21GMo12-1	Chr12_126100	2.58	0.0727					
	q21GMo12-2	Chr12_18278484	3.70	***0.0117***					

QTLs shown in bold italic indicate an FDR ≤ 0.05

natural selection within the minimum acceptable levels necessary for survival. In other words, as this trait was not emphasized until very recently in modern rice breeding, it is expected that many alleles contributing to the fine-tuning of elemental content are hidden within breeding populations.

We created a MAGIC population from multiple crosses of eight high-yielding rice varieties in Japan (Ogawa et al. 2018a). Novel phenotypes that circumvent the tradeoffs between grain length and width were identified in this population (Ogawa et al. 2018b). This feature is unique compared to conventional single-cross populations. In this study, we conducted a genome-wide association study (GWAS) on the concentrations of 13 elements in rice grain and straw using this MAGIC population. This study has two objectives. The first is to utilize the unique characteristics of the MAGIC population to elucidate the genetic basis of variation in elemental concentration in rice. The second is to promote the effective exploration of candidate genes that affect this trait in breeding populations.

Materials and Methods

Materials and Field Test

A scheme for the development of the 8-way MAGIC population (Ogawa et al. 2018a) is shown in Supplementary Fig.S1. Eight founders representing high-yield varieties in Japan–Hokuriku 193 (HO), Mizuhochikara (MI), Suweon 258 (SU), Akidawara (AK), Takanari (TK), Bekogonomi (BE), Ruriaoba (RU), and Tachiaoba (TC)–were selected as founders of the MAGIC population. Four two-way hybrids (AB, CD, EF, and GH) were generated, followed by two four-way hybrids (ABCD and EFGH) and two eight-way F_1 hybrids (ABCDEFGH). The 182 lines of the MAGIC population (F_{10}) and their eight founders were planted in 2019 (sown on May 20, transplanted on June 20) and 2021 (sown on May 19, transplanted on June 19) at the experimental field of the Institute of Plant Science and Resources, Okayama University (34° 35' 31" N and 133° 46' 7" E), Kurashiki, Japan. Plants were grown in two adjacent plots within the same field; straw samples were collected from one plot, and grain samples were collected from the other plot. In each plot, six plants were planted in each of the four rows, resulting in a total of 24 plants. To determine the appropriate time for sampling, the days to heading were recorded for all lines. Heading was defined as the stage at which the panicle of the highest culm emerged at least 2 cm from the flag-leaf sheath.

Measurement of Element Contents

The straw at the flowering stage and grain at the mature stage were sampled and subjected to elemental analysis. After drying, the grain was hulled to obtain brown rice. The straw was dried at 70 °C for 24 h, and ground into a

fine powder. Brown rice and dried powder (around 0.2 g) of the straw were taken and digested with nitric acid at a concentration of 61% for 10 to 15 h in a thermostatic metal bath (Dry Thermo Unit) at a temperature of up to 135 °C. The samples were filled with ultrapure water prior to analysis. The concentrations of 13 elements (P, K, Ca, Mg, As, Cd, Cr, Cu, Fe, Mo, Mn, Ni, and Zn) were determined using inductively coupled plasma mass spectrometry (ICP-MS; 7700X, Agilent Technologies, Santa Clara, CA, USA) in the helium mode.

Data Visualization

The correlation coefficient matrix heatmap was generated using Chiplot (Ji et al. 2022; Li et al. 2023), and the frequency distribution plot and box plot were produced using the "ggplot2" package in R (Wickham 2010). Manhattan plots were drawn using the "CMplot" package (Yin et al. 2021). QTL genetic maps derived from the MAGIC population were constructed using MapChart version 2.32 (Voorrips 2002).

Statistical Analysis

All statistical analyses were performed using the R software version 4.2.3 (R Core Team 2018). Standard functions such as *cor()* and *aov()* from the built-in stats package were used to conduct correlation analysis and one-way ANOVA, respectively, with the significance threshold set at $p < 0.05$. The quantitative data of the elements across different years were standardized using z-score normalization prior to model fitting. The statistical significance of differences among the means was assessed using the Tukey–Kramer multiple comparison test.

GWAS and QTL Definition

Haplotype data corresponding to 13,603 SNPs in the MAGIC population have been reported by Ogawa et al. (2018a). Haplotype prediction followed the method used for the Arabidopsis MAGIC population (Kover et al. 2009). Associations between the imputed genotype and phenotype data for all 13 elements in the MAGIC population were analyzed using the Kruskal–Wallis test to calculate *p*-values. *P*-values were obtained for the sample types of grain and straw in 2021 (Table 1) using GWAS. To control for false positives, *p*-values were adjusted using the Benjamini–Hochberg (BH) method implemented in the p.adjust() function, and the resulting adjusted *p*-values were interpreted as false discovery rate (FDR)-controlled *q*-values. The experiment was conducted with pre-set thresholds of FDR ≤ 0.1 and FDR ≤ 0.05, and QTL screening was performed accordingly. QTLs were named using the following convention: "q" followed by the last two digits of the year (21), sample type (G for grain, S for straw), elemental symbols, and chromosome numbers (e.g., *q21GCd12* and *q21SMg4*).

Candidate Gene Estimation by Haplotype Comparison

Candidate gene estimation was performed near the QTL regions identified by the GWAS. After setting the threshold as noted in the previous section, all SNP loci were considered "significant" in this study when FDR ≤ 0.1. We conducted keyword searches in the Oryzabase (Yamazaki et al. 2010) and RAP-DB (Sakai et al. 2013) databases using three types of keywords and commonly studied agronomic traits. The element-related keywords consisted of the element name alone and in combination with the terms "ion" and "transporter" (e.g., "cadmium," "cadmium ion," and "cadmium transporter"). In addition, searches were performed using trait-related terms such as "heading date", "tiller number", and "detoxification". Gene information related to keywords, including OsID, was downloaded and merged into a single file. Furthermore, genes located within QTL peak regions were also considered candidates even without keyword-based annotations if they satisfied criteria: (1) they exhibited significant phenotypic differences among haplotype groups based on multiple comparisons, and (2) their genotype patterns were identical to or similar to those of nearby screened genes. Additionally, for the screened genes, information such as gene location, functional description, or publication of the OsID was retrieved from the RAP-DB. Polymorphic information of the screened genes among the eight founders was obtained using TASUKE+ (Kumagai et al. 2019). By sorting the polymorphisms in the genetic information, the haplotypes of the eight founders were classified into several groups. Mean trait values were calculated for each of the eight founder alleles and each classified haplotype group, and then multiple comparisons using Tukey–Kramer tests were performed to confirm the relationship between the haplotype groups and phenotypic values. If a significant difference was observed between groups, the gene was considered a candidate gene.

Results

General Profiles of Element Concentration in Straw and Grain

We compared the trends of 13 element concentrations (P, K, Ca, Mg, As, Cd, Cr, Cu, Fe, Mo, Mn, Ni, and Zn) in grain measured in 2019 and 2021 (Supplementary Tables S1, S2, and S3). We observed a positive correlation between the years except for Cr in grain (Supplementary Fig. S2 A and B), indicating that environmental differences across the years did not substantially affect the relative accumulation patterns. This consistency indicates that the MAGIC population is suitable for the genetic analysis of grain element concentrations. The present

study focused on conducting further analyses of the 2021 data set.

Descriptive statistics of the 13 element concentrations in both the MAGIC population and founders are summarized. Mean elemental concentrations differed markedly between grain and straw: most elements were higher in straw than in grain, whereas Mg and P were slightly higher in grain, and Cd was strongly enriched in grain (Supplementary Tables S4 and S5). Overall, the MAGIC lines exhibited wider value ranges across most elements than the founders. To further evaluate phenotypic variability, coefficients of variation (CV) were calculated. In grain, the CV of most elements was higher in the MAGIC population than in the founders (Supplementary Table S4), indicating increased variability in the MAGIC population. In contrast, other elements (P, Mn, Fe, Ni, and Mo) showed slightly higher CV values in the founder group. Similar patterns were also observed in straw (Supplementary Table S5). In addition to the previously mentioned elements, P, Mn, and Fe exhibited noticeably higher CVs in the MAGIC population. These results demonstrate a general expansion of phenotypic variation in the MAGIC population compared to the founders. The distributions showed continuous variation with transgressive segregants, indicating that the traits of the elements were governed by polygenic controls (Supplementary Fig. S3).

Distinct Correlation Patterns of Elemental Concentrations in Grain and Straw

To investigate the relationship between the elemental accumulation in straw and grain, we performed Pearson's correlation analysis of the concentrations of the 13 elements in the MAGIC population (Supplementary Table S6). The results reveal a wide range of correlation coefficients (r), indicating varying degrees of element translocation and partitioning between the vegetative and reproductive organs. Among these, Ca, As, and Mo exhibited relatively strong positive correlations. Other elements exhibited weak or negligible correlations.

Next, we calculated the correlation coefficients for all pairs of the 13 elements in grain and straw. In grain (Fig. 1A), days to heading were positively correlated with Cd ($r = 0.68$), Ni ($r = 0.46$), and Mn ($r = 0.39$), and negatively correlated with As ($r = -0.59$), Mo ($r = -0.45$), Fe ($r = -0.37$), Zn ($r = -0.30$), Mg ($r = -0.32$), and

P ($r = -0.32$). Among the elemental pairs, the strongest positive correlation was found between Mg and P ($r = 0.86$), followed by Zn–P ($r = 0.70$), Zn–Fe ($r = 0.65$), and Cd–Ni ($r = 0.62$). In addition, significant positive correlations were observed between Cu and Zn ($r = 0.56$), Cu and Fe ($r = 0.54$), and Mn and Ca ($r = 0.58$). Conversely, distinct negative correlations were evident between Cd and As ($r = -0.55$), Cd and Mo ($r = -0.34$), and As and Ni ($r = -0.44$). These correlation trends were consistent with the grain data from 2019 (Supplementary Fig. S4).

In the straw (Fig. 1B), the correlation patterns differed partially from those observed in the grain, although some similarities existed. For instance, correlations between days to heading and both Cd ($r = -0.02$) and Ni ($r = -0.02$) were negligible in straw, whereas negative correlations with Mo ($r = -0.46$) and As ($r = -0.37$) were like those observed in grain. Generally, positive correlations were dominant among the element pairs, with the highest observed between Cr and Ni ($r = 1.00$), followed by Cr–Cu ($r = 0.74$) and Cr–Fe ($r = 0.71$). A clear correlation cluster was identified between Fe, Ni, and Cu (Fe–Ni: $r = 0.70$, Ni–Cu: $r = 0.73$, and Fe-Cu: $r = 0.58$). Mn exhibited a distinct positive correlation with Cd ($r = 0.62$) and Mg ($r = 0.56$). Importantly, the correlation between Mg and P ($r = 0.36$) was markedly weaker compared with grain ($r = 0.86$). Moreover, strong negative correlations found in grain, such as Cd–As, were only weakly negative ($r = -0.11$) in straw, further highlighting sample-type-specific relationships.

The integration of these findings indicates that the correlation between "elements" (or between "elements" and "days to heading") manifests differently across sample types. It is noteworthy that elements such as Cd, Mg, and P demonstrate divergent correlations with other elements when comparing straw and grain.

QTLs Detection in the MAGIC Population

At a GWAS significance threshold of FDR ≤ 0.1, 53 QTLs for five elements (Cd, Cu, Fe, Mn, Mo) in grain, and 51 QTLs for four elements (Ca, Mg, Mn, Mo) in straw were detected (Fig. 2; Table 1). Specifically, grain QTLs included Cd (15 loci), Cu (9), Fe (19), Mn (1), and Mo (9), whereas straw QTLs included Ca (11), Mg (20), Mn (9), and Mo (11). Although QTLs for Mn and Mo were found in both the grain and the straw, no common regions were found. No QTLs were detected for other elements in the straw (P, K, As, Cd, Cr, Cu, Fe, Ni, and Zn) or grain (P, K, Ca, Mg, As, Cr, Ni, and Zn) at the specified thresholds (Supplementary Fig. S5). The detected QTLs were distributed across all the chromosomes, with the highest density observed on chromosome 6, where 19 QTLs were detected for seven elements (Ca, Cd, Cu, Fe, Mg, Mn, and Mo). In contrast, only four QTLs for the three elements were found on chromosomes 8 (Mo, Mg, and Fe), 9 (Cd, Mg, and Mo), and 10 (Mg, Ca, and Mo) (Fig. 3; Table 1). Nineteen QTL clusters formed by overlapping multiple significant QTL regions were observed across all chromosomes, except for chromosomes 5 and 12 (Fig. 3; Supplementary Table S7).

To identify more significant regions from a total of the 104 detected QTLs, the threshold was tightened to FDR ≤ 0.05, reducing the total number of significant

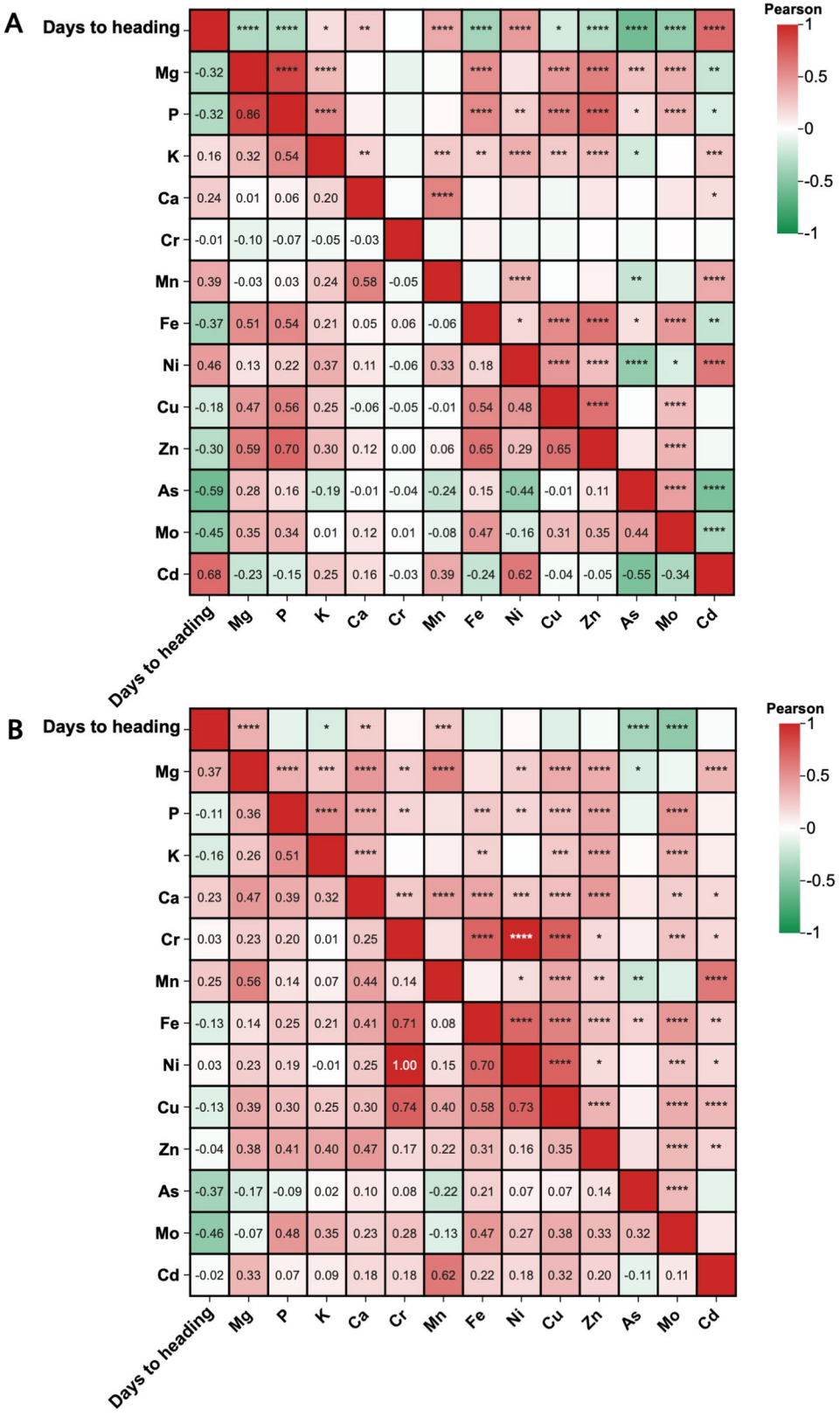

Fig. 1 Correlation coefficient matrix between the 13 elements and days to heading in the MAGIC population. Matrix heat maps were made based on the data for (**A**) grain and (**B**) straw. According to the Pearson coefficient (r), red indicates a positive correlation, while green indicates a negative correlation. The intensity of the color reflects the strength of the correlation. The bottom-left and top-right sections of the matrix display the correlation coefficients and significance levels (****: 0.0001, ***: 0.001, **: 0.01, and *: 0.05, respectively).

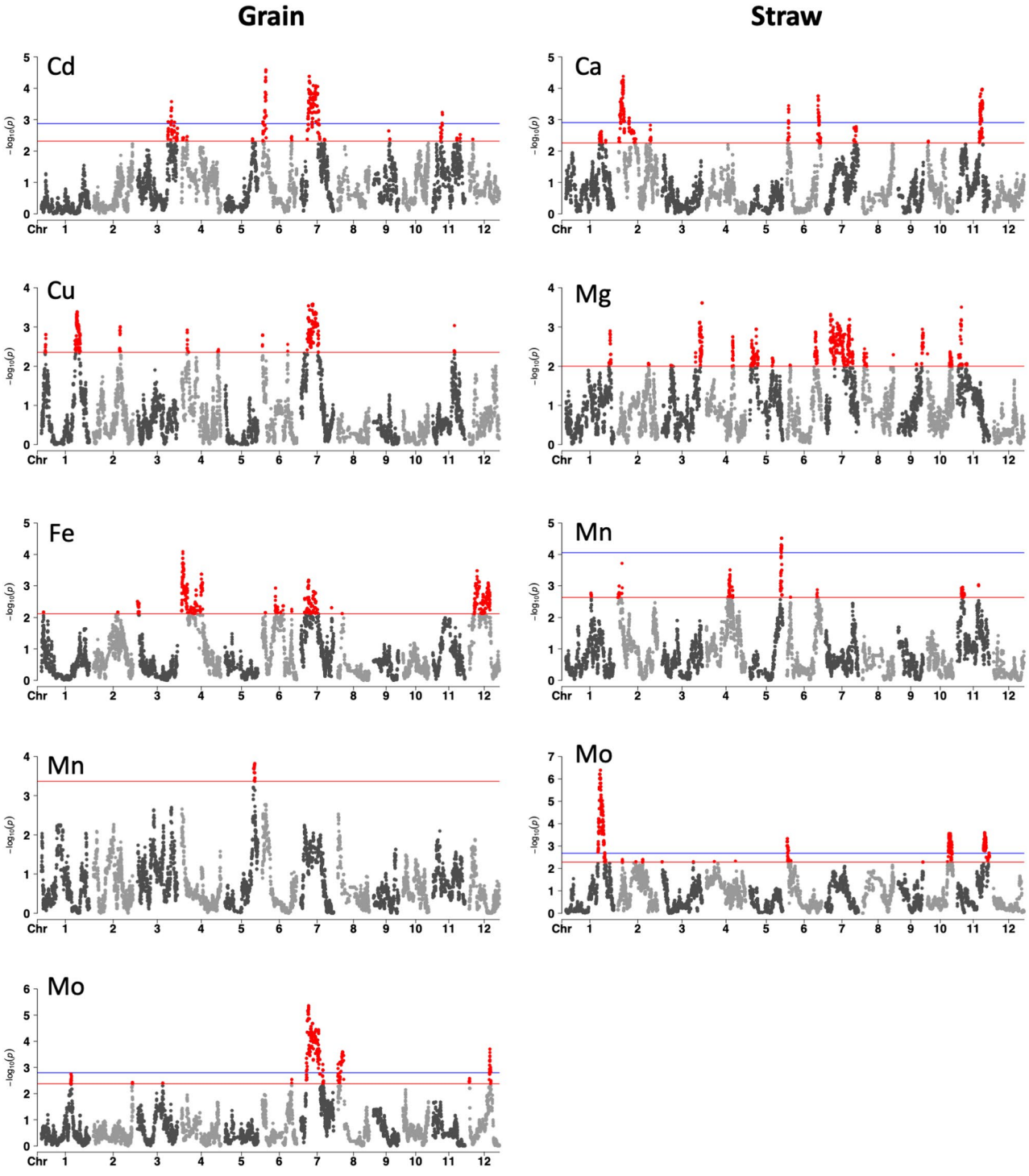

Fig. 2 Manhattan plots of the significant QTLs. The left and right panels show Manhattan plots for grain and straw, respectively. The horizontal axis indicates the chromosome names, and the vertical axis shows the $\log_{10}(P)$ value. The red and blue horizontal lines denote the significance thresholds at FDR = 0.1 and FDR = 0.05, respectively. Data points exceeding the FDR threshold of 0.1 are highlighted in red.

QTLs to 10 across grain and straw (Table 1). In the grain, six Cd QTLs were detected on chromosomes 3, 6, 7, and 11, and four Mo QTLs were identified on chromosomes 7, 8, and 12. In straw, five Ca QTLs were found on chromosomes 2, 6, and 11, one Mn QTL on chromosome 5, and four Mo QTLs on chromosomes 1, 6, 10, and 11. The most significant QTLs included *q21SMo1* ($-\log_{10}(p) = 6.39$), *q21GMo7-1* (5.36), *q21GCd6-2* (4.58), and *q21SMn5* (4.52) (Table 1).

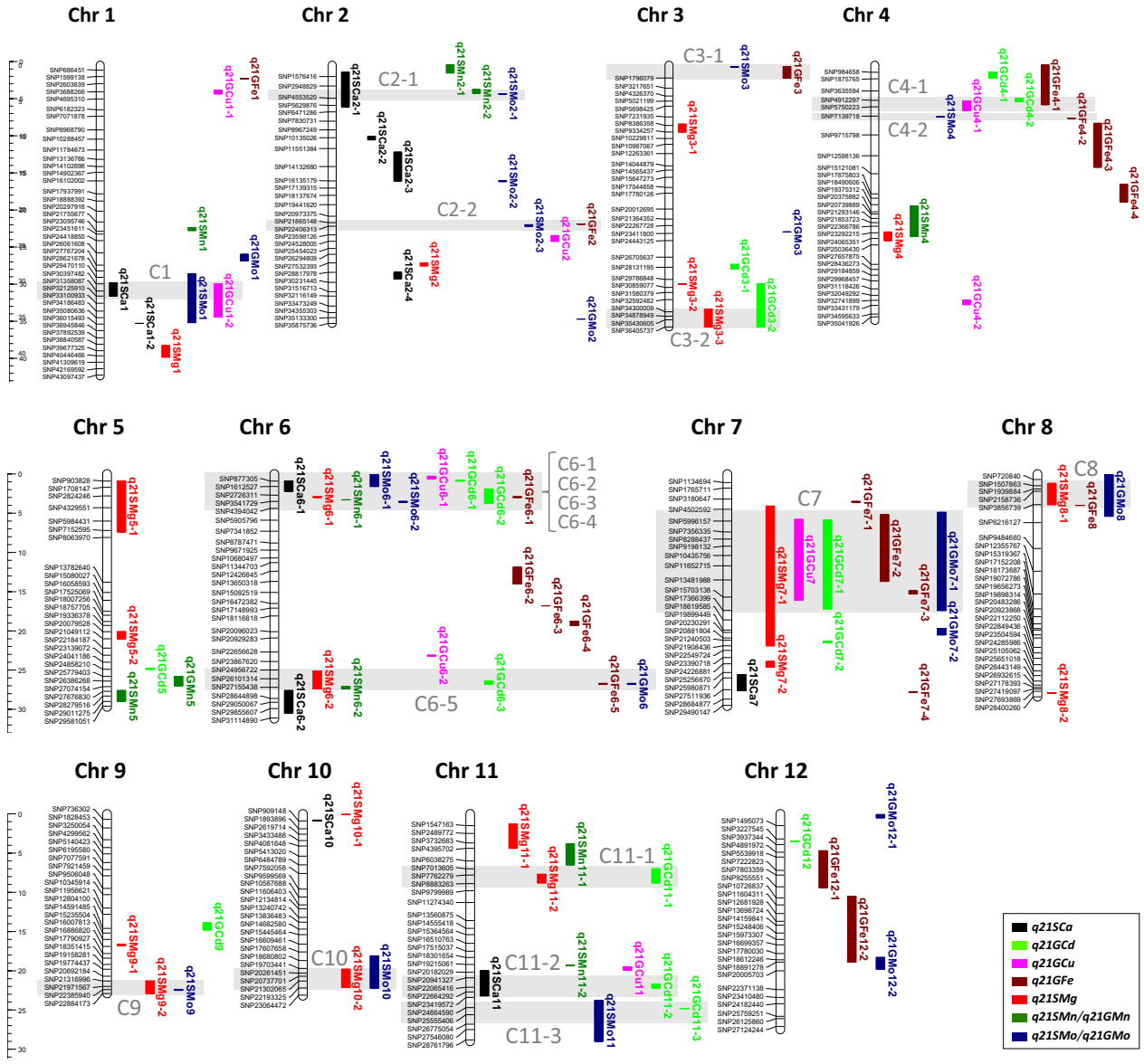

Fig. 3 Distributions of the 104 significant QTLs on rice physical map. The physical positions were referenced from IRGSP 1.0 (Kawahara et al. 2013). A threshold of FDR ≤ 0.1 was applied. The numbers on the left side of each chromosome indicate the physical positions (Mb) of 342 representative SNP loci selected at approximately equal distances from the 13,603 SNP loci. The bars on the right side of each chromosome represent the QTL regions, with different colors denoting various elements. In the QTL names, the prefix "q" is followed by "21" to indicate the sampling year (2021), "G" for grain, and "S" for straw. The grey shaded region indicates a QTL cluster formed by the partial overlap of multiple QTLs, and the gray letters beginning with "C" indicate the corresponding QTL cluster in Supplementary Table S7.

Prioritization of Candidate Genes Based on Haplotype Information

Among the genes screened using the keywords, we compared founder haplotypes and phenotypic data for 430 genes located within the detected 104 QTL regions. In total, 52 genes distributed across 15 QTLs related to the six elements exhibited concordant changes in both haplotypes and phenotypes (Table 2).

Several of the 52 candidate genes have been reported to be associated with elemental accumulation. Among them, the *q21GMo8* region includes *OsMOT1;1* (*Os08g0101500*), which encodes a molybdate transporter significantly associated with Mo accumulation (Huang et al. 2019). We first selected the SNP site closest to *OsMOT1;1* and performed multiple comparison analysis using the haplotype of the eight founders and the Mo concentration data of 182 lines in the MAGIC population (Fig. 4A). Subsequently, sequence variations in *OsMOT1;1* in the eight founders were analyzed using TASUKE+. Two deletions (2 bp at positions 642–643 and 7 bp at positions 646–652) were identified in the transcript of *OsMOT1;1* specifically in the founder HO,

Table 2 Candidate genes estimated from the consistency between phenotypic values and haplotype variations of the eight founder varieties

Element	QTL name	Chr.	PVE[*1)]	Gene	OsID	Description and (Ref#)[*2)]	Hap1	Hap2	Hap3	Most probable SnpEff	Nucleotide and amino acid change (from AK Hap to others)	Sup. Fig. S6[*3)]
	q21SCa2-1	2	11.2	*OsACA9*	*Os02g0176700*	Similar to autoinhibited calcium ATPase (Meng et al. 2015)	HO, RU, SU	TK	AK, BE, MI, TC	missense_variant	c.58G > A|p.Asp20Asn	Figure 4. DEF
				OsHSL3	*Os02g0320800*	Similar to Iron/ascorbate-dependent oxidoreductase (Kawahara et al. 2013)	HO, RU, SU, TK	AK, BE, MI, TC		stop_lost	c.907T > C|p.Ter303Argext*?	1
Ca	*q21SCa2-3*	2	13.7	*OsCAX1c*	*Os02g0314300*	Sodium/calcium exchanger membrane region domain containing protein (Huynh et al. 2018)	HO, RU, SU, TK	AK, BE, MI, TC		missense_variant	c.409 A > C|p.Ile137Leu	2
				OsPP2C14	*Os02g0471500*	Protein phosphatase 2 C domain containing protein (Kover et al. 2009)	HO, RU, SU	TK	AK, BE, MI, TC	missense_variant	c.605G > A|p.Ser202Asn	3
	q21SCa11	11	9.0	*OsCML6*	*Os11g0586200*	Similar to Calmodulin (Bandillo et al. 2013)	HO, RU, SU, TK	BE, TC	AK, MI	splice_donor_variant&intron_variant	c.326 + 1G > A	Figure 4. GHI
	q21GCd6-2	6	15.8	*OsWAK61*	*Os06g0142500*	Similar to Wall-associated kinase 3 (Pasion et al. 2023)	RU	AK, BE, HO, MI, SU, TC, TK		frameshift_variant&start_lost	c.−9_17delGGCCATCCGATGGGAGCCTTAGTACT	4
				OsCDT2	*Os06g0143100*	Similar to Cadmium tolerant 1 (Huang et al. 2012)	RU	AK, BE, HO, MI, SU, TC, TK		missense_variant	c.27 C > A|p.Asp9Glu	5

Table 2 (continued)

Element	QTL name	Chr.	PVE[*1)]	Gene	OsID	Description and (Ref#)[*2)]	Hap1	Hap2	Hap3	Most probable SnpEff	Nucleotide and amino acid change (from AK Hap to others)	Sup. Fig. S6[*3)]
				SPDT	*Os06g0143700*	SULTR-like phosphorus distribution transporter (Ogawa et al. 2018)	RU	AK, BE, HO, MI, SU, TC, TK		missense_variant	c.140 C > T|p.Ala47Val	6
				OsPLL6	*Os06g0144200*	Similar to Pectate lyase homolog (EC 4.2.2.2) (R Core Team 2018)	RU	AK, BE, HO, MI, SU, TC, TK		missense_variant	c.1321 A > G|p.Thr441Ala	7
Cd				*OsPLL7*	*Os06g0144900*	Pectate lyase/Amb allergen domain containing protein (R Core Team 2018)	RU	AK, BE, HO, MI, SU, TC, TK		missense_variant	c.976 C > A|p.Arg326Ser	8
	q21GCd7-1	7	9.9	*OsZIP8*	*Os07g0232800*	Zinc transporter, Zn uptake and distribution (Huang et al. 2019)	HO, MI, RU, SU	TK	AK, BE, TC	conservative_inframe_deletion	c.481_486delACCGCC|p.Thr161_Ala162del	9
				HMA3	*Os07g0232900*	Root-to-shoot cadmium (Cd) translocation (Ma and Yamaji 2006)	HO, RU, TK	MI, SU	AK, BE, TC	missense_variant		10
				OsNramp1	*Os07g0258400*	Integral membrane protein, Metal ion transport (Cavanagh et al. 2008)	HO, MI, RU, SU, TK	AK, BE, TC		splice_acceptor_variant&3_prime_UTR_variant&intron_variant	c.*298-1_*339delAAATATAAATGTAAATAAATGCAGTTAAAGTAACACCTTGCTC	11

Table 2 (continued)

Element	QTL name	Chr.	PVE[*1)]	Gene	OsID	Description and (Ref#)[*2)]	Hap1	Hap2	Hap3	Most probable SnpEff	Nucleotide and amino acid change (from AK Hap to others)	Sup. Fig. S6[*3)]
Cu	*q21GCu2*	2	13.9	*OsPP2C22*	*Os02g0607500*	Putative protein phosphatase 2 C 22 (Ogawa et al. 2018)	RU	HO, TK	AK, BE, MI, SU, TC	stop_gained	c.1348G > T|p.Glu450*	12
	q21GCu7	7	9.0	*OsTFIIS*	*Os07g0229700*	Similar to DNA-directed RNA polymerase I subunit 12 (Kathpalia 2018)	HO, MI, RU, SU, TK	AK, BE, TC		missense_variant	c.250G > A|p.Ala84Thr	13
				OsCYB5-14	*Os07g0232200*	Similar to Flavohemoprotein b5/b5R variant (Li et al. 2023)	HO, MI, RU, SU, TK	AK, BE, TC		missense_variant	c.157G > A|p.Ala53Thr	14
				DRM2	*Os03g0110800*	DNA methyltransferase, Vegetative and reproductive development (Khush 2005)	RU	AK, BE, HO, MI, SU, TC, TK		missense_variant	c.1217 A > G|p.His406Arg	15
				OsF5HL2	*Os03g0112900*	Similar to Aldehyde 5-hydroxylase (Hawkesford 2012)	RU	AK, BE, HO, MI, SU, TC, TK		missense_variant	c.427G > C|p.Val143Leu	16
				TK	*Os03g0113100*	Similar to Thymidine kinase (Mackay et al. 2014)	RU	AK, BE, HO, MI, SU, TC, TK		disruptive_inframe_insertion	c.161_163dupCGG|p.Ala54dup	17
	q21GFe3	3	12.0	*OsCd1*	*Os03g0114800*	Major facilitator superfamily protein, Cd uptake, Grain Cd accumulation (Orasen et al. 2025)	RU	AK, BE, HO, MI, SU, TC, TK		missense_variant	c.1346T > A|p.Val449Asp	18

Table 2 (continued)

Element	QTL name	Chr.	PVE[*1)]	Gene	OsID	Description and (Ref#)[*2)]	Hap1	Hap2	Hap3	Most probable SnpEff	Nucleotide and amino acid change (from AK Hap to others)	Sup. Fig. S6[*3)]
				Os-ENODL10	*Os03g0115000*	Cupredoxin domain containing protein (Dell'Acqua et al. 2015)	RU	AK, BE, HO, MI, SU, TC, TK		missense_variant	c.344T > C|p.Leu115Pro	19
Fe				*OsHIPP27*	*Os03g0126700*	Similar to Barley stem rust resistance protein (Codex 2025)	RU	AK, BE, HO, MI, SU, TC, TK		disruptive_inframe_insertion	c.346_347insACGACGGCGACGGCAAGAAGG|p.Lys115_Gly116insAspAsp-GlyAspGlyLysLys	20
				CIPK9	*Os03g0126800*	Regulation of ammonium-dependent root growth (Miyadate et al. 2011)	RU	AK, BE, HO, MI, SU, TC, TK		frameshift_variant	c.1243delC|p.Leu415fs	21
				OsCDPK7	*Os03g0128700*	Calcium-dependent protein kinase, isoform 11 (EC 2.7.1.-) (CDPK 11) (Pascual et al. 2015)	RU	AK, BE, HO, MI, SU, TC, TK		missense_variant	c.1420G > A|p.Val474Ile	22
				OsCYB5-14	*Os07g0232200*	Similar to Flavohemoprotein b5/b5R variant (Li et al. 2023)	HO, MI, RU, SU, TK	AK, BE, TC		missense_variant	c.157G > A|p.Ala53Thr	23
	q21GFe7-2	7	11.3		*Os07g0291750*	Electron carrier/heme binding/iron ion binding/monooxygenase	HO, MI, RU, SU, TK	AK, BE, TC		missense_variant	c.113G > A|p.Arg38Lys	24
					Os07g0292100	Similar to CYP71B6 (CYTOCHROME P450 71B6)	HO, MI, RU, SU, TK	AK, BE, TC		frameshift_variant	c.388_394delAAACTGG|p.Lys130fs	25

Table 2 (continued)

Element	QTL name	Chr.	PVE[*1)]	Gene	OsID	Description and (Ref#)[*2)]	Hap1	Hap2	Hap3	Most probable SnpEff	Nucleotide and amino acid change (from AK Hap to others)	Sup. Fig. S6[*3)]
Mg	*q21SMg3-3*	3	13.2	*2-ODD26*	*Os03g0856000*	2OG-Fe(II) oxygenase domain containing protein (Boonburapong and Buaboocha 2007)	HO, MI, RU, SU, TK	AK, BE, (TC)		frameshift_variant	c.306_307delCG|p.Asp103fs	26
				OsHMP23	*Os03g0861400*	Hypothetical conserved gene (Codex 2025)	HO, MI, RU, SU, TK	AK, BE, (TC)		disruptive_inframe_insertion	c.990_992dupCCA|p.His330dup	27
	q21SMg8-1	8	10.9	*OsP0A*	*Os08g0130500*	Similar to 60 S acidic ribosomal protein p0 (Chang et al. 2020)	HO, RU, TK	AK, BE, TC, MI, SU		missense_variant	c.770 A > G|p.Glu257Gly	28
				OsTFIIS	*Os07g0229700*	Similar to DNA-directed RNA polymerase I subunit 12 (EC 2.7.7.6) (Kathpalia 2018)	HO, MI, RU, SU, TK	AK, BE, TC		missense_variant	c.250G > A|p.Ala84Thr	29
				OsCYB5-14	*Os07g0232200*	Similar to Flavohemoprotein b5/b5R variant (Li et al. 2023)	HO, MI, RU, SU, TK	AK, BE, TC		missense_variant	c.157G > A|p.Ala53Thr	30
				HMA3	*Os07g0232900*	Root-to-shoot cadmium (Cd) translocation (Ma and Yamaji 2006)	HO, RU, TK	MI, SU	AK, BE, TC	missense_variant		31
				OsNramp1	*Os07g0258400*	Similar to Metal transporter (Cavanagh et al. 2008)	HO, MI, RU, SU, TK	AK, BE, TC		splice_acceptor_variant&3_prime_UTR_variant&intron_variant	c.*298-1_*339delAAATATAAATGTAAATAAATGCAGTTAAAGTAACACCTTGCTC	32

Table 2 (continued)

Element	QTL name	Chr.	PVE[*1)]	Gene	OsID	Description and (Ref#)[*2)]	Hap1	Hap2	Hap3	Most probable SnpEff	Nucleotide and amino acid change (from AK Hap to others)	Sup. Fig. S6[*3)]
	q21GMo7-1	7	12.0	*OsC3H49*	*Os07g0281000*	Nucleotide-binding, alpha-beta plait domain containing protein	HO, MI, RU, SU, TK	AK, BE, TC		missense_variant	c.1097 C > A|p.Thr366Lys	33
				OsPARP1	*Os07g0413700*	Response to DNA damage, gametophyte development, promotion of seed setting rate (Islam et al. 2016)	HO, MI, RU, SU, TK	AK, BE, TC		missense_variant	c.138 A > C|p.Leu46Phe	34
				OsCesA3	*Os07g0424400*	Similar to Cellulose synthase-7 (Mangino et al. 2022)	HO, MI, RU, SU, TK	AK, BE, TC		missense_variant	c.537G > A|p.Met179Ile	35
				XBOS34	*Os07g0446100*	Zinc finger, RING/FYVE/PHD-type domain containing protein	HO, MI, RU, SU, TK	AK, BE, TC		missense_variant	c.887T > A|p.Leu296Gln	36
Mo	*q21GMo8*	8	13.1	*OsMOT1;1*	*Os08g0101500*	Molybdate transporter, Uptake and translocation of molybdate (Gebert et al. 2009)	HO	SU(Hap2),TK(Hap3),RU(Hap4),TC(Hap5)	AK, BE, MI(Hap6)	frameshift_variant	c.642_643delGC|p.Gln215fs c.646_652delCAGCAGC|p.Gln216fs	Figure 4. ABC
				NADP-ME2	*Os01g0723400*	NADP-malic enzyme, salt and osmotic stress tolerance, disease resistance (Kumagai et al. 2019)	HO, RU, SU, TK	BE	AK, MI, TC	frameshift_variant	c.19_20insCG|p.Val7fs	37

Table 2 (continued)

Element	QTL name	Chr.	PVE[*1)]	Gene	OsID	Description and (Ref#)[*2)]	Hap1	Hap2	Hap3	Most probable SnpEff	Nucleotide and amino acid change (from AK Hap to others)	Sup. Fig. S6[*3)]
				RD22	*Os01g0733500*	Similar to Dehydration-induced protein RD22-like protein 1 (Descalsota-Empleo et al. 2019)	RU, HO, TK, SU	AK, BE, MI, TC		missense_variant	c.1009G > A|p.Ala337Thr	38
				OsPFK02	*Os01g0738800*	Conserved hypothetical protein (Kojima et al. 2002)	HO, RU, TK, SU	AK, BE, MI, TC		missense_variant	c.77T > C|p.Val26Ala	39
					Os01g0739000	Similar to Mitochondrial processing peptidase	HO, RU, TK, SU	AK, BE, MI, TC		missense_variant	c.50 A > C|p.Tyr17Ser	40
				OscytME3	*Os01g0743500*	Cytosolic NADP malic enzyme (Chen et al. 2022)	HO, RU, TK, SU	AK, BE, MI, TC		missense_variant	c.796 A > C|p.Asn266His	41
	q21SMo1	1	15.4	*OsGATA6*	*Os01g0745700*	Positive regulation of panicle development and grain number, regulation of grain size (Pingali 2012)	HO, RU, TK, SU	AK, BE, MI, TC		missense_variant	c.994 C > T|p.His332Tyr	42
				NUP85	*Os01g0746200*	Nucleoporin, Common symbiosis signaling (SYM) pathway (Duan et al. 2017)	HO, RU, TK, SU	AK, BE, MI, TC		missense_variant	c.1243G > A|p.Gly415Arg	43
				OsCESA4	*Os01g0750300*	Cellulose synthase catalytic subunit, secondary cell wall formation (International Rice Genome Sequencing Project 2005)	HO, RU, TK, SU	AK, BE, MI, TC		missense_variant	c.221 C > T|p.Ala74Val	44

Table 2 (continued)

Element	QTL name	Chr.	PVE[*1)]	Gene	OsID	Description and (Ref#)[*2)]	Hap1	Hap2	Hap3	Most probable SnpEff	Nucleotide and amino acid change (from AK Hap to others)	Sup. Fig. S6[*3)]
				NBIP1	*Os01g0755700*	RING-type E3 ubiquitin ligase, Regulation of phosphate and nitrate signalling (Evenson and Gollin 2003)	RU, TK	AK, BE, HO, MI, SU, TC		missense_variant	c.233T>C|p.Val78Ala	45
				OsHMP6	*Os01g0758000*	Similar to copper-binding family protein (Codex 2025)	RU	HO, TK, SU	AK, BE, MI, TC	disruptive_inframe_deletion	c.297_305delACACGCAGC|p.His100_Ala102del	46
				OsCIPK30	*Os01g0759200*	CBL-interaction protein kinase protein, Resistance to Rice stripe virus (RSV) disease (Ji et al. 2022)	RU	HO, TK, SU	AK, BE, MI, TC	missense_variant	c.499G>A|p.Gly167Ser	47
				OsPK7	*Os01g0759400*	OsPK7 (Os01t0759400-02)	RU, HO, TK, SU	AK, BE, MI, TC		missense_variant	c.780T>G|p.Asn260Lys	48
	q21SMo10	10	13.6	*OsHIPP25*	*Os10g0532300*	Heavy metal transport/detoxification protein domain containing protein (Codex 2025)	SU	AK, BE, HO, MI, TC, TK, RU		disruptive_inframe_deletion	c.270_293delCGGCGGCGGCGACGGCAAGAAGGA|p.Asp90_Lys97del	49

[*1)]PVE (phenotypic variance explained) was calculated as the coefficient of determination (R^2) from a linear model fitting the phenotype to the marker haplotype/genotype (phenotype ~ marker). PVE is reported as $100 \times R^2$

[*2)]The reference papers supporting the description are listed under their corresponding numbers in Supplementary Information S8

[*3)]The figure index of results of multi-haplotype comparison in Supplemental Fig. S6

both annotated as high-impact frameshift mutations by SnpEff. (Fig. 4B). In addition, moderate-impact mutations were detected in HO, RU, SU, TC, and TK, whereas no moderate- or higher-impact mutations were found in AK, BE, or MI. Based on these variation patterns, we grouped the eight founders into six haplotypes, Hap1 (HO), Hap2 (SU), Hap3 (TK), Hap4 (RU), Hap5 (TC), and Hap6 (AK, BE, and MI, respectively, with no more than moderate mutations), followed by a multiple comparison analysis (Fig. 4C). The results show that Hap1 had a significantly lower Mo content than Hap6, whereas the Mo content of Hap2 to Hap5 (carrying moderate-impact mutations) showed intermediate values. These data suggest that natural variations in *OsMOT1;1* affect the accumulation of Mo in grain.

Within the *q21SCa2-1* region, we predicted *OsACA9* (*Os02g0176700*), a novel candidate gene encoding an auto-inhibited calcium ATPase that may be involved in Ca transport (Wang X et al. 2024). Using the same approach, we performed founder haplotype-based analysis (Fig. 4D). In the investigation of sequence variation across the founders, six moderate-impact variants were identified in HO, RU, and SU (Hap1); three moderate SNPs were detected in TK (Hap2); and no moderate or higher impact mutations were found in AK, BE, MI, and TC (Hap3) (Fig. 4E). Multiple comparisons across the three haplotypes revealed that Hap1 had a significantly lower Ca content than Hap3, whereas that of Hap2 was intermediate (Fig. 4F). This result supports *OsACA9* potentially involved in the natural variation in Ca accumulation in straw.

Interestingly, the candidate genes listed in Table 2 also include genes not previously associated with the relevant elements. For example, within *q21SCa11*, we predicted *OsCML6* (*Os11g0586200*), a gene encoding a calmodulin-like protein (Boonburapong and Buaboocha 2007), was a potential regulator of Ca accumulation. Multiple comparison analyses showed that AK and MI had significantly lower Ca concentrations than the other treatments (Fig. 4G). High-impact splice donor variants were detected in BE, HO, RU, SU, TC, and TK (Fig. 4H). Four additional moderate-impact SNPs were also identified. Further analysis revealed that a moderate SNP at position 348 bp was present in HO, RU, SU, and TK, whereas an SNP at 47 bp was present in BE and TC. Therefore, we grouped the founders as Hap1 (HO, RU, SU, and TK), Hap2 (BE and TC), and Hap3 (AK and MI without moderate- or high-impact variants) (Fig. 4H). The comparison among haplotype groups revealed that Hap1 and Hap2, which carry splice donor or moderate-impact mutations, exhibited significantly higher Ca content than Hap3, with no significant difference between Hap1 and Hap2 (Fig. 4I). This result implies that the splice donor variant of *OsCML6* may enhance gene function or expression by altering splicing efficiency, thereby increasing Ca accumulation in the straw.

Taken together, the integration of SnpEff annotation, sequence variant analysis, and haplotype–phenotype association of multiple founders enables the MAGIC population to accurately narrow down candidate genes associated with elemental accumulation. The results of all the other candidate genes are shown in Supplementary Figs. S6-1 to S6-49.

Discussion

Effectiveness and Considerations for the MAGIC Population

Multi-parent advanced generation inter-cross (MAGIC) populations provide an effective platform for dissecting complex quantitative traits because they combine multiple founder genomes and accumulate recombination events across generations. Compared with conventional biparental populations and diversity panels, MAGIC populations increase genetic diversity caused by recombination among multiple founder alleles. This improves the resolution of genetic dissection of complex traits. Consistent with previous studies using MAGIC populations (Wang P. et al. 2024; Zhi et al. 2023), our MAGIC population redetected known genetic loci and highlighted additional candidate regions. For example, *q21GMo8* co-localized with the previously reported Mo transporter gene *OsMOT1;1*, and *q21SCa2-1* mapped near the Ca-related ATPase *OsACA9*. Importantly, we also detected loci that have not been emphasized in prior studies, such as *q21SCa11*, in which *OsCML6* represents a plausible candidate gene (Fig. 4).

It is important to note that because eight founder alleles were assumed in this MAGIC population, the number of lines representing each genotype was smaller than that in a biparental population of the same size. Consequently, the statistical power to detect QTLs may be reduced, resulting in higher p-values despite similar levels of phenotypic variation. To reduce the risk of false negatives, we applied a relatively permissive significance threshold (FDR ≤ 0.10) during the initial QTL detection stage (Table 1). Candidate genes were subsequently prioritized using haplotype comparisons and polymorphism analyses among founder alleles. Although this does not negate the ability of the MAGIC population to perform GWAS at a high resolution, larger population sizes are preferable for sensitivity and detection purposes.

Relationship Between Element Accumulation and Days to Heading Based on QTL Distribution

The accumulation of elements in rice is influenced by both the genetic background and environmental factors, among which flowering time (i.e., days to heading) is a key trait affecting elemental accumulation (Duan et al. 2017; Descalsota et al. 2019). In the present study, days

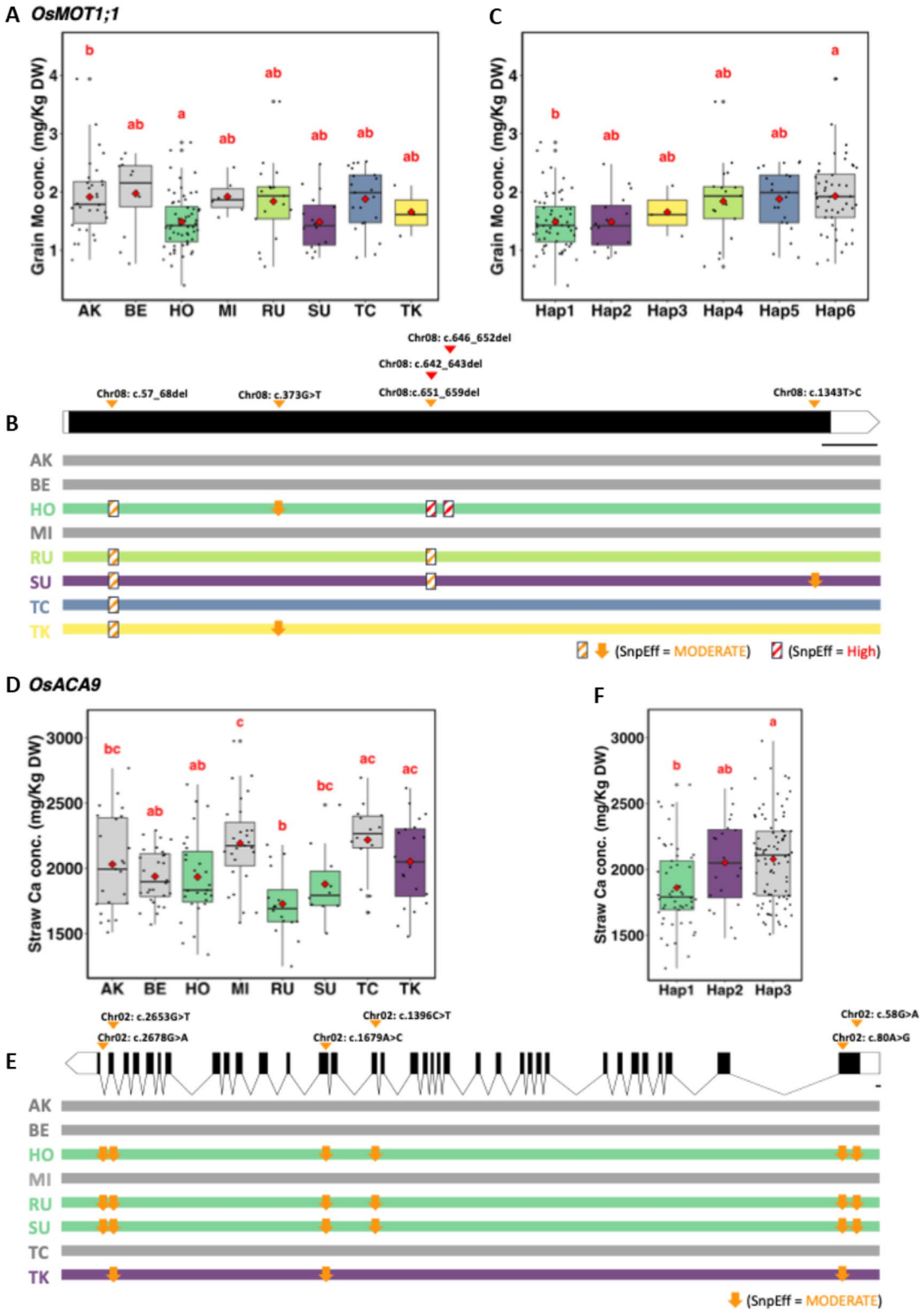

Fig. 4 Genetic structure and multiple haplotype comparison for *OsMOT1;1*, *OsACA9*, and *OsCML6* that are candidate genes of the three QTLs: *q21GMo8*, *q21SCa2-1*, and *q21SCa11*. (**A**), (**D**), and (**G**) show the results of multiple comparisons among eight haplotypes. The red rhombus in each boxplot represents the mean value of the group. The red letters indicate statistically significant differences. (**B**), (**E**), and (**H**) show the gene structure and haplotype variations of *OsMOT1;1*, *OsACA9*, and *OsCML6*, respectively. Yellow and red arrows represent SNPs and the corresponding diagonal squares indicate deletions with moderate and high predicted SnpEff effects, respectively. (**C**), (**F**), and (**I**) show the results of multiple comparisons among haplotype groups based on sequence variation. The meanings of the red rhombus and letters are the same as those in (**A**), (**D**), and (**G**).

to heading were significantly positively correlated with grain Cd concentration ($r = 0.68$, Fig. 1A). Previous findings have suggested that late-flowering rice genotypes tend to accumulate more Cd (Yamamoto et al. 2024), likely because of extended root uptake periods and prolonged element translocation.

Further, QTL mapping supported a genetic contribution to the observed association (Figs. 2 and 3). At the short-arm end of chromosome 6, two QTLs for grain Cd accumulation (*q21GCd6-1* and *q21GCd6-2*) were mapped close to the flowering-time regulators *Hd3a* (*Os06g0157700*) and *RFT1* (*Os06g0157500*) (Kojima et al. 2002). However, grain Cd accumulation is strongly influenced by the bioavailability of Cd in soil and associated field conditions. This proximity does not necessarily indicate a direct causal role of flowering genes in Cd transport or accumulation. Instead, the signal may reflect linkage with nearby Cd-related loci, or an indirect effect whereby heading date alters the timing and duration of plant exposure to soil Cd availability and redox dynamics during grain filling. In addition, several other elements showed a QTL cluster in the same region on chromosome 6 (Fig. 3; Supplementary Table S7), including Mo (*q21SMo6-1*, *q21SMo6-2*), Fe (*q21GFe6-1*), Cu (*q21GCu6-1*), Mn (*q21SMn6-1*), Mg (*q21SMg6-1*), and Ca (*q21SCa6-1*). Collectively, these patterns are consistent with a genomic region enriched for element QTLs, although whether this reflects shared regulators, tightly linked loci, or pleiotropic effects mediated by developmental or environmental responsiveness requires further validation.

A similar trend was observed for chromosome 7. The grain Cd QTL (*q21GCd7-1*) mapped near *Ghd7* (*Os07g0261200*), a major regulator of days to heading and plant architecture (Xue et al. 2008). As discussed above, this proximity could reflect either a tight linkage to Cd-related loci or an indirect association mediated by developmental timing. In addition, QTLs for Mo (*q21GMo7-1*), Fe (*q21GFe7-2*), Cu (*q21GCu7*), and Mg (*q21SMg7-1*) were identified in this region (Fig. 3; Supplementary Table S7). This suggests the existence of a genetic cluster that jointly influences the days to heading and the accumulation of multiple elements.

Relationship of Element Accumulation Between Grain and Straw Based on QTL Distribution

We demonstrated a clear difference in the correlation structures between straw and grain (Fig. 1), mapped 104 QTLs to the rice genome (Fig. 3), and grouped them into 19 QTL clusters (Supplementary Table S7). Integrating these data revealed that several element pairs showing high correlations within the sample significantly overlapped with specific QTL clusters. These results suggest that these regions harbor genetic factors that jointly regulate transport, allocation, and specific accumulation.

In the straw, the positive correlation of Mo–Ca (chromosome 1, C1), moderate correlation of Mn–Ca (chromosome 2, C2-1), and strong correlation of Mn–Mg (chromosomes 6, C6) coincided with their corresponding QTL clusters. This phenotypic correlation and genetic co-localization pattern suggest that these regions may contain pleiotropic genes that simultaneously regulate the accumulation of two elements or tightly linked loci with coordinated effects. Notably, the C6-5 region on chromosome 6 is a QTL-enriched hotspot and overlaps with a strong Mn–Mg correlation region. This region contains candidate genes related to Mg transport, such as members of the *MRS2/MGT* family (Gebert et al. 2009), suggesting a potential mechanistic link. Nevertheless, direct evidence for a shared transporter or causal gene affecting both elements is still lacking and requires further validation.

In contrast, a different pattern was observed in the grain. The C7 region on chromosome 7 showed positive correlations of Mo–Fe and Mo–Cu, along with a negative correlation of Mo–Cd. This complex relationship is likely attributable to the combined actions of developmental regulators and metal transporters. As mentioned in the previous section, the *Ghd7* gene, which is involved in the days to heading, may have contributed to this. In addition, this region contains major metal transporters. *OsHMA3* (*Os07g0232900*), a vacuolar Cd transporter, determines Cd sequestration, and loss-of-function alleles significantly increase Cd translocation to grain, whereas functional alleles can effectively reduce Cd accumulation (Miyadate et al. 2011; Ueno et al. 2010). Furthermore, *OsNRAMP5* (*Os07g0257200*), a major transporter of Mn/Cd uptake in the roots, is induced under Fe deficiency (Chang et al. 2020; Sasaki et al. 2012). This provides a mechanistic explanation for the antagonistic relationships among Mo, Fe, and Cd. Thus, the C7 cluster can be considered a regulatory hub. Here, *Ghd7*-mediated developmental effects determine the source–sink balance, whereas specific metal transporters govern the selective partitioning of ions. This mechanistic separation likely underlies the observed Mo–Fe–Cu synergy and Mo–Cd antagonism.

Validity of the Estimated Candidate Genes

This study integrated SnpEff annotation, structural variant analysis, and haplotype–phenotype association to predict 52 candidate genes for 15 QTL regions associated with six elements. The MAGIC population, which includes multiple founder SnpEff information, was well-suited for this integrated analysis, enabling the prioritization of known and novel candidate genes underlying elemental accumulation. These candidates were related to

six elements: Ca (5 genes), Cd (8), Cu (3), Fe (11), Mg (3), and Mo (22) (Fig. 4; Table 2; Supplementary Fig. S6). This strategy not only confirmed several previously reported functional genes, such as *OsMOT1;1* and *OsACA9*, but also identified novel candidates, including *OsCML6*, thereby offering new insights into the genetic regulation of elemental accumulation in rice. For *OsMOT1;1* and *OsACA9*, distinct types of mutations—including frameshift and missense variants—were significantly associated with Mo and Ca concentrations, respectively (Fig. 4ABC; Fig. 4DEF). Notably, the splice donor site variant of *OsCML6* was positively correlated with Ca levels, suggesting its possible role in modulating gene expression through altered splicing efficiency (Fig. 4GHI), thereby influencing Ca homeostasis.

Two well-characterized heavy-metal transporter genes, *OsHMA3* (Supplementary Fig. S6–10), and *OsNRAMP1* (*Os07g0258400*) (Supplementary Fig. S6–11) were estimated within the Cd-associated QTL region on chromosome 7 (*q21GCd7-1*). Haplotype analysis of the eight MAGIC parents revealed structural variants of *OsHMA3* in HO, MI, RU, SU, and TK, whereas AK, BE, and TC lacked moderate- or high-impact mutations. Multiple comparisons showed that lines carrying the mutated alleles exhibited significantly higher grain Cd concentrations, supporting previous findings that loss-of-function mutations in *OsHMA3* enhance Cd translocation to the grain. A similar trend was observed for *OsNRAMP1*. Collectively, this study not only validated known metal transporter genes under natural allelic variation but also proposed novel regulatory candidate alleles.

Application of the Rice MAGIC Population for Improving Elemental Accumulation Under Different Soil Conditions

Our MAGIC population, consisting of multiple founder alleles, is particularly well-suited for broadly detecting genotype × environment (G×E) interactions within cultivated rice species. Although the present study was conducted under single soil conditions, phenotypic assessments and GWAS of MAGIC across diverse soil environments are expected to advance our understanding of the mechanisms underlying elemental accumulation in nature. For example, Orasen et al. (2025) conducted an ionomics GWAS under contrasting water management conditions, revealing that most marker–trait associations were specific to the conditions. We also evaluated the accumulation patterns of 13 elements in straw at the heading stage and in grain at maturity under acidic, neutral, and alkaline soil pH conditions using eight founders of this MAGIC population (Yamamoto et al. 2024). This experiment suggests that there are element-specific interactions between genotype, soil pH, and flowering time, highlighting the importance of investigating the genetic basis underlying these interactions. Building upon these findings, performing a GWAS of MAGIC across contrasting soil conditions could provide a more robust genetic foundation for understanding nutrient adaptation under stressful environments in rice and support the identification of genes with broad-spectrum or environment-specific advantages.

Furthermore, from the perspective of gene network research on element accumulation, utilizing MAGIC populations with high haplotype resolution holds the potential to rapidly translate large-scale ionomics information into practical breeding objectives (Tiozon et al. 2024). Furthermore, integrating predicted candidate gene sets into regulatory networks or gene-element network models may reveal shared pathways between elements and potential hub regulators (Pasion et al. 2023). Overall, this study provides a dataset and analytical framework that serve as a foundation for molecular breeding.

Conclusions

This study highlights the unique advantages of multiparental MAGIC populations for dissecting complex traits such as elemental accumulation in rice. Unlike biparental populations, MAGIC offers broad genetic diversity and high recombination, enabling the detection of moderate-effect loci and improving mapping resolution. We provided a comprehensive overview of genetic variation in the uptake and accumulation of 13 elements in rice grain and straw, revealing extensive phenotypic diversity and sample-type-specific correlations. By integrating GWAS with haplotype-based analysis, we predicted candidate genes involved in the uptake and partitioning of essential and toxic elements, including both known transporters and novel regulators. These findings provide a strong genetic foundation for breeding programs aimed at enhancing nutrient efficiency and stress tolerance. Future work should focus on functional validation of these genes and their incorporation into genomic selection strategies to accelerate rice improvement under diverse environmental conditions.

Abbreviations

AK	Akidawara
As	Arsenic
B	Boron
BE	Bekogonomi
C	Carbon
Ca	Calcium
Cd	Cadmium
Cl	Chlorine
Cr	Chromium
Cu	Copper
CV	Coefficient of variation
FDR	False discovery rate
Fe	Iron
GWAS	Genome-wide association study
G×E	Genotype by environment interaction
Hg	Mercury
HO	Hokuriku 193
ICP-MS	Inductively coupled plasma mass spectrometry

K	Potassium
MAGIC	Multi-parent advanced generation inter-cross
Mg	Magnesium
MI	Mizuhochikara
Mn	Manganese
Mo	Molybdenum
N	Nitrogen
Ni	Nickel
OsID	*Oryza sativa* ID
P	Phosphorus
Pb	Lead
QTL	Quantitative trait loci
RU	Ruriaoba
Si	Silicon
SNP	Single nucleotide polymorphism
SU	Suweon 258
TC	Tachiaoba
TK	Takanari
Zn	Zinc

Supplementary Information

The online version contains supplementary material available at https://doi.org/10.1186/s12284-026-00908-6.

Supplementary Material 1

Supplementary Material 2

Supplementary Material 3

Acknowledgements
We acknowledge the Groups of Integrated Genome Breeding, Plant Stress Physiology, Mrs. Sanae Rikiishi, and Mr. Makoto Ishii for their assistance with the experiments.

Author Contributions
TY designed the study. QZ, TY, and KK conducted the experiments. DO, JY, and TY developed the plant materials. QZ, TF, DO, JY, and TY analyzed the data. JFM assisted and supervised ICP-MS experiments. QZ wrote the manuscript and TY edited and revised it. All the authors have read and approved the final version of the manuscript.

Funding
This work was supported in part by JSPS KAKENHI Grants-in-Aid for Scientific Research 20H02958 to TY, 16H06296 and 21H05034 to JFM, the China Scholarship Council Program (Project ID: 202305080109), and the Ohara Scholarship Foundation.

Data Availability
All data generated or analyzed during this study are included in this published article and its supplementary information files.

Declarations

Ethics Approval and Consent to Participate
Not applicable.

Consent for Publication
Not applicable.

Competing Interests
The authors declare no competing interests.

Received: 9 January 2026 / Accepted: 1 April 2026
Published online: 11 May 2026

References

Bandillo N, Raghavan C, Muyco PA, Sevilla MA, Lobina IT, Dilla-Ermita CJ, Tung CW, McCouch S, Thomson M, Mauleon R, Singh RK, Gregorio G, Redoña E, Leung H (2013) Multi-parent advanced generation inter-cross (MAGIC) populations in rice: progress and potential for genetics research and breeding. Rice (N Y) 6(1). https://doi.org/10.1186/1939-8433-6-11

Boonburapong B, Buaboocha T (2007) Genome-wide identification and analyses of the rice calmodulin and related potential calcium sensor proteins. BMC Plant Biol 7. https://doi.org/10.1186/1471-2229-7-4

Cavanagh C, Morell M, Mackay I, Powell W (2008) From mutations to MAGIC: resources for gene discovery, validation and delivery in crop plants. Curr Opin Plant Biol 11:215–221. https://doi.org/10.1016/j.pbi.2008.01.002

Chang JD, Huang S, Yamaji N, Zhang WW, Ma JF, Zhao FJ (2020) *OsNRAMP1* transporter contributes to cadmium and manganese uptake in rice. Plant Cell Environ 43:2476–2491. https://doi.org/10.1111/pce.13843

Chen R, Deng Y, Ding Y, Guo J, Qiu J, Wang B, Wang C, Xie Y, Zhang Z, Chen J, Chen L, Chu C, He G, He Z, Huang X, Xing Y, Yang S, Xie D, Liu Y, Li J (2022) Rice functional genomics: decades' efforts and roads ahead. Sci China Life Sci 65:33–92. https://doi.org/10.1007/s11427-021-2024-0

Codex Alimentarius Commission (2025) General Standard for Contaminants and Toxins in Food and Feed (CXS 193–1995) https://www.fao.org/fileadmin/user_upload/agns/pdf/CXS_193e.pdf (Accessed on March 7, 2026)

Dell'Acqua M, Gatti DM, Pea G, Cattonaro F, Coppens F, Magris G, Hlaing AL, Aung HH, Nelissen H, Baute J, Frascaroli E, Churchill GA, Inzé D, Morgante M, Pè ME (2015) Genetic properties of the MAGIC maize population: a new platform for high definition QTL mapping in *Zea mays*. Genome Biol 16(1). https://doi.org/10.1186/s13059-015-0716-z

Descalsota-Empleo GI, Amparado A, Inabangan-Asilo MA, Tesoro F, Stangoulis J, Reinke R, Swamy BPM (2019) Genetic mapping of QTL for agronomic traits and grain mineral elements in rice. Crop J 7(4):560–572. https://doi.org/10.1016/j.cj.2019.03.002

Duan G, Shao G, Tang Z, Chen H, Wang B, Tang Z, Yang Y, Liu Y, Zhao FJ (2017) Genotypic and environmental variations in grain cadmium and arsenic concentrations among a panel of high yielding rice cultivars. Rice 10(1). https://doi.org/10.1186/s12284-017-0149-2

Evenson RE, Gollin D (2003) Assessing the impact of the green revolution, 1960 to 2000. Science 300(5620):758–762. https://doi.org/10.1126/science.1078710

Gebert M, Meschenmoser K, Svidová S, Weghuber J, Schweyen R, Eifler K, Lenz H, Weyand K, Knoop V (2009) A root-expressed magnesium transporter of the MRS2/MGT gene family in Arabidopsis thaliana allows for growth in low-Mg^{2+} environments. Plant Cell 21(12):4018–30. https://doi.org/10.1105/tpc.109.070557

Hawkesford M, Horst W, Kichey T, Lambers H, Schjoerring J, Møller IS, White P (2012) Functions of macronutrients. Marschner's Element Nutrition of Higher Plants (3rd ed.). 135–189. https://doi.org/10.1016/B978-0-12-384905-2.00006-6

Huang BE, George AW, Forrest KL, Kilian A, Hayden MJ, Morell MK, Cavanagh CR (2012) A multiparent advanced generation inter-cross population for genetic analysis in wheat. Plant Biotechnol J 10(7):826–839. https://doi.org/10.1111/j.1467-7652.2012.00702.x

Huang XY, Liu H, Zhu YF, Pinson SRM, Lin HX, Guerinot ML, Zhao FJ, Salt DE (2019) Natural variation in a molybdate transporter controls grain molybdenum concentration in rice. New Phytol 221(4):1983–1997. https://doi.org/10.1111/nph.15546

Huynh BL, Ehlers JD, Huang BE, Muñoz-Amatriaín M, Lonardi S, Santos JRP, Ndeve A, Batieno BJ, Boukar O, Cisse N, Drabo I, Fatokun C, Kusi F, Agyare RY, Guo YN, Herniter I, Lo S, Wanamaker SI, Xu S, Close TJ, Roberts PA (2018) A multi-parent advanced generation inter-cross (MAGIC) population for genetic analysis and improvement of cowpea (*Vigna unguiculata* L. Walp.). Plant J 93(6):1129–1142. https://doi.org/10.1111/tpj.13827

International Rice Genome Sequencing Project (2005) The map-based sequence of the rice genome. Nature 436:793–800. https://doi.org/10.1038/nature03895

Islam MS, Thyssen GN, Jenkins JN, Zeng L, Delhom CD, McCarty JC, Deng DD, Hinchliffe DJ, Jones DC, Fang DD (2016) A MAGIC population-based genome-wide association study reveals functional association of *GhRBB1_A07* gene with superior fiber quality in cotton. BMC Genomics 17(1). https://doi.org/10.1186/s12864-016-3249-2

Ji X, Tang J, Zhang J (2022) Effects of salt stress on the morphology, growth and physiological parameters of *Juglansmicrocarpa* L. seedlings. Plants 11(18). https://doi.org/10.3390/plants11182381

Kathpalia R, Bhatla SC (2018) Plant Mineral Nutrition. In: Plant Physiology, Development and Metabolism. Springer, Singapore. https://doi.org/10.1007/978-981-13-2023-1_2

Kawahara Y, de la Bastide M, Hamilton JP, Kanamori H, McCombie WR, Ouyang S, Schwartz DC, Tanaka T, Wu J, Zhou S, Childs KL, Davidson RM, Lin H, Quesada-Ocampo L, Vaillancourt B, Sakai H, Lee SS, Kim J, Numa H, Itoh T, Buell CR, Matsumoto T (2013) Improvement of the *Oryza sativa* Nipponbare reference genome using next generation sequence and optical map data. Rice 6. https://doi.org/10.1186/1939-8433-6-4

Khush GS (2005) What it will take to feed 5.0 billion rice consumers in 2030. Plant Mol Biol 59(1):1–6. https://doi.org/10.1007/s11103-005-2159-5

Kojima S, Takahashi Y, Kobayashi Y, Monna L, Sasaki T, Araki T, Yano M (2002) *Hd3a*, a rice ortholog of the *Arabidopsis FT* gene, promotes transition to flowering downstream of *Hd1* under short-day conditions. Plant Cell Physiol 43(10):1096–1105. https://doi.org/10.1093/pcp/pcf156

Kover PX, Valdar W, Trakalo J, Scarcelli N, Ehrenreich IM, Purugganan MD, Durrant C, Mott R (2009) A multiparent advanced generation inter-cross to fine-map quantitative traits in Arabidopsis thaliana. PLoS Genet 5(7). https://doi.org/10.1371/journal.pgen.1000551

Kumagai M, Nishikawa D, Kawahara Y, Wakimoto H, Itoh R, Tabei N, Tanaka T, Itoh T (2019) TASUKE+: a web-based platform for exploring GWAS results and large-scale resequencing data. DNA Res 26(6):445–452. https://doi.org/10.1093/dnares/dsz029

Li X, Li J, Zhao Q, Qiao L, Wang L, Yu C (2023) Physiological, biochemical, and genomic elucidation of the *Ensifer adhaerens* M8 strain with simultaneous arsenic oxidation and chromium reduction. J Hazard Mater 441. https://doi.org/10.1016/j.jhazmat.2022.129862

Mackay IJ, Bansept-Basler P, Barber T, Bentley AR, Cockram J, Gosman N, Greenland AJ, Horsnell R, Howells R, O'Sullivan DM, Rose GA, Howell PJ (2014) An eight-parent multiparent advanced generation inter-cross population for winter-sown wheat: creation, properties, and validation. G3 (Bethesda) 4(9):1603–1610. https://doi.org/10.1534/g3.114.012963

Ma JF, Yamaji N (2006) Silicon uptake and accumulation in higher plants. Trends Plant Sci 11(8):392–397. https://doi.org/10.1016/j.tplants.2006.06.007

Mangino G, Arrones A, Plazas M, Pook T, Prohens J, Gramazio P, Vilanova S (2022) Newly developed MAGIC population allows identification of strong associations and candidate genes for anthocyanin pigmentation in eggplant. Front Plant Sci 13. https://doi.org/10.3389/fpls.2022.847789

Meng L, Li H, Zhang L, Wang JK (2015) QTL icimapping: integrated software for genetic linkage map construction and quantitative trait locus mapping in biparental populations. Crop J 3(3):269–283. https://doi.org/10.1016/j.cj.2015.01.001

Miyadate H, Adachi S, Hiraizumi A, Tezuka K, Nakazawa N, Kawamoto T, Katou K, Kodama I, Sakurai K, Takahashi H, Satoh-Nagasawa N, Watanabe A, Fujimura T, Akagi H (2011) OsHMA3, a P_{1B}-type of ATPase affects root-to-shoot cadmium translocation in rice by mediating efflux into vacuoles. New Phytol 189(1):190–199. https://doi.org/10.1111/j.1469-8137.2010.03459.x

Ogawa D, Yamamoto E, Ohtani T, Kanno N, Tsunematsu H, Nonoue Y, Yano M, Yamamoto T, Yonemaru JI (2018a) Haplotype-based allele mining in the Japan-MAGIC rice population. Sci Rep 8(1). https://doi.org/10.1038/s41598-018-22657-3

Ogawa D, Nonoue Y, Tsunematsu H, Kanno N, Yamamoto T, Yonemaru JI (2018b) Discovery of QTL alleles for grain shape in the Japan-MAGIC rice population using haplotype information. G3 Genes Genomes Genet 8(11):3559–3565. https://doi.org/10.1534/g3.118.200558

Orasen G, Mica E, Lucchini G, Negrini N, Nocito FF, Baldoni E, Tondelli A, Valè G, Sacchi GA (2025) A genome-wide association study of the grain ionome in rice *Oryza Sativa* ssp. *Japonica* under two diverse water management systems. Rice 18. https://doi.org/10.1186/s12284-025-00847-8

Pascual L, Desplat N, Huang BE, Desgroux A, Bruguier L, Bouchet JP, Le QH, Chauchard B, Verschave P, Causse M (2015) Potential of a tomato MAGIC population to decipher the genetic control of quantitative traits and detect causal variants in the resequencing era. Plant Biotechnol J 13(4):565–577. https://doi.org/10.1111/pbi.12282

Pasion EA, Misra G, Kohli A, Sreenivasulu N (2023) Unraveling the genetics underlying micronutrient signatures of diversity panel present in brown rice through genome–ionome linkages. Plant J 113:749–771. https://doi.org/10.1111/tpj.16080

Pingali PL (2012) Green Revolution: Impacts, limits, and the path ahead. Proc Natl Acad Sci USA 109(31):12302–12308. https://doi.org/10.1073/pnas.0912953109

R Core Team (2018) R: A Language and Environment for Statistical Computing. R Foundation for Statistical Computing, Vienna

Sakai H, Lee SS, Tanaka T, Numa H, Kim J, Kawahara Y, Wakimoto H, Yang CC, Iwamoto M, Abe T, Yamada Y, Muto A, Inokuchi H, Ikemura T, Matsumoto T, Sasaki T, Itoh T (2013) Rice Annotation Project Database (RAP-DB): an integrative and interactive database for rice genomics. Plant Cell Physiol 54(2):e6. https://doi.org/10.1093/pcp/pcs183

Sannemann W, Huang BE, Mathew B, Léon J (2015) Multi-parent advanced generation inter-cross in barley: high-resolution quantitative trait locus mapping for flowering time as a proof of concept. Mol Breed 35:86. https://doi.org/10.1007/s11032-015-0284-7

Sasaki A, Yamaji N, Yokosho K, Ma JF (2012) Nramp5 is a major transporter responsible for manganese and cadmium uptake in rice. Plant Cell 24(5):2155–2167. https://doi.org/10.1105/tpc.112.096925

Taiz L, Zeiger E, Møller IM, Murphy A (2015) Mineral Nutrition. In: Plant Physiology and Development, 6th ed. Sinauer Associates. ISBN: 978-1-60535-255-8

Tiozon RN, Buenafe RJQ, Jain V, Sen P, Molina LR, Anacleto R, Sreenivasulu N (2024) Machine learning technique unraveled subspecies specific ionomic variation with the preferential mineral enrichment in rice. Cereal Chem 101:367–381. https://doi.org/10.1002/cche.10706

Uchimiya M, Bannon D, Nakanishi H, McBride MB, Williams MA, Yoshihara T (2020) Chemical speciation, plant uptake, and toxicity of heavy metals in agricultural soils. J Agric Food Chem 68(46):12856–12869. https://doi.org/10.1021/acs.jafc.0c00183

Ueno D, Yamaji N, Kono I, Huang CF, Ando T, Yano M, Ma JF (2010) Gene limiting cadmium accumulation in rice. Proc Natl Acad Sci USA 107(38):16500–16505. https://doi.org/10.1073/pnas.1005396107

Voorrips RE (2002) Mapchart: software for the graphical presentation of linkage maps and QTLs. J Hered 93(1):77–8. https://doi.org/10.1093/jhered/93.1.77

Wang P, Yang Y, Li D, Yu Z, Zhang B, Zhou X, Xiong L, Zhang J, Wang L, Xing Y (2024) Powerful QTL mapping and favorable allele mining in an all-in-one population: a case study of days to heading. Nat Sci Rev 11(8). https://doi.org/10.1093/nsr/nwae222

Wang X, Wang Z, Lu Y, Huang J, Hu Z, Lou J, Fan X, Gu Z, Liu P, Ma B, Chen X (2024) OsACA9, an autoinhibited Ca^{2+}-ATPase, synergically regulates disease resistance and leaf senescence in rice. Int J Mol Sci 25(3). https://doi.org/10.3390/ijms25031874

Wickham H (2010) A layered grammar of graphics. J Comput Graph Stat 19(1):3–28. https://doi.org/10.1198/jcgs.2009.07098

Xue W, Xing Y, Weng X, Zhao Y, Tang W, Wang L, Zhou H, Yu S, Xu C, Li X, Zhang Q (2008) Natural variation in *Ghd7* is an important regulator of days to heading and yield potential in rice. Nat Genet 40(6):761–767. https://doi.org/10.1038/ng.143

Yamamoto T, Kashihara K, Furuta T, Zhang Q, Yu E, Ma JF (2024) Genetic background influences mineral accumulation in rice straw and grains under different soil pH conditions. Sci Rep 14(1). https://doi.org/10.1038/s41598-024-66036-7

Yamamoto T, Yonemaru J, Yano M (2009) Towards the understanding of complex traits in rice: substantially or superficially? DNA Res 16(3):141–154. https://doi.org/10.1093/dnares/dsp006

Yamazaki Y, Sakaniwa S, Tsuchiya R, Nonomura K, Kurata N (2010) Oryzabase: an integrated information resource for rice science. Breed Sci 60(5):544–548. https://doi.org/10.1270/jsbbs.60.544

Ye C, Zheng G, Tao Y, Xu Y, Chu G, Xu C, Chen S, Liu Y, Zhang X, Wang D (2024) Effect of soil texture on soil nutrient status and rice nutrient absorption in paddy soils. Agronomy 14(6):1339. https://doi.org/10.3390/agronomy14061339

Yin L, Zhang H, Tang Z, Xu J, Yin D, Zhang Z, Yuan X, Zhu M, Zhao S, Li X, Liu X (2021) rMVP: a memory-efficient, visualization-enhanced, and parallel-accelerated tool for genome-wide association study. Genom Proteom Bioinform 19(4):619–628. https://doi.org/10.1016/j.gpb.2020.10.007

Yonemaru J, Yamamoto T, Ebana K, Yamamoto E, Nagasaki H, Shibaya T, Yano M (2012) Genome-wide haplotype changes produced by artificial selection during rice breeding in Japan. PLoS One 7(3). https://doi.org/10.1371/journal.pone.0032982

Zhi S, Zou W, Li J, Meng L, Liu J, Chen J, Ye G (2023) Mapping QTLs and gene validation studies for Mg2+ uptake and translocation using a MAGIC population in rice. Front Plant Sci 14. https://doi.org/10.3389/fpls.2023.1131064

Publisher's Note